Ferromagnetic resonance study of magnetic order-disorder phase transition in amorphous $Fe_{90-x}Co_xZr_{10}$ alloys

S. N. Kaul and P. D. Babu
School of Physics, University of Hyderabad, Central University P.O., Hyderabad 500 134, India
(Received 24 April 1991; revised manuscript received 22 July 1991)

The utility of the ferromagnetic-resonance (FMR) technique to determine accurately the spontaneous magnetization and initial susceptibility critical exponents β and γ, which characterize the ferromagnetic (FM) -paramagnetic (PM) phase transition at the Curie temperature T_C for ferromagnetic materials is demonstrated through a detailed comparative study on amorphous $Fe_{90}Zr_{10}$ alloy, which involves bulk magnetization and FMR measurements performed on the same sample in the critical region. Magnetization data deduced from the FMR measurements taken on amorphous $Fe_{90-x}Co_xZr_{10}$ alloys with $x=0$, 1, 2, 4, 6, and 8 in the critical region satisfy the magnetic equation of state characteristic of a second-order phase transition. Contrary to the anomalously large values of the exponents β and γ reported earlier, the present values, $\beta=0.38\pm0.03$ and $\gamma=1.38\pm0.06$, are *composition-independent* and match very well the three-dimensional Heisenberg values. The fraction of spins that actually participates in the FM-PM phase transition, c, is found to increase with the Co concentration as $c(x)-c(0)\cong ax^2$ and possess a small value of 11% for the alloy with $x=0$. The "peak-to-peak" FMR linewidth (ΔH_{pp}) varies with temperature in accordance with the empirical relation $\Delta H_{pp}(T)=\Delta H(0)+[A/M_s(T)]$, where M_s is the saturation magnetization. Both the Landé splitting factor g as well as the Gilbert damping parameter λ are *independent* of temperature, but, with increasing Co concentration (x), λ decreases slowly while g stays constant at a value 2.07 ± 0.02.

I. INTRODUCTION

The ferromagnetic- (FM) paramagnetic (PM) phase transition in amorphous (*a*-) $Fe_{90+x}Zr_{10-x}$ and $Fe_{90-x}(Co,Ni)_xZr_{10}$ alloys has become a controversial[1] issue ever since the bulk magnetization (BM) measurements[2,3] in the critical region on these alloys have yielded values for the spontaneous magnetization and "zero-field" susceptibility critical exponents β and γ that are roughly 1.4 *times larger* than the renormalization-group estimates[4] for an isotropic nearest-neighbor (NN) three-dimensional (3D) Heisenberg ferromagnet primarily because the unphysically large values for critical exponents have been taken to reflect large fluctuation in the exchange interaction. Subsequently, an elaborate analysis[1,5] (reanalysis) of high-precision magnetization data on *a*-$Fe_{90}Zr_{10}$ (published[2,6] data on *a*-$Fe_{91}Zr_9$ and *a*-$Fe_{92}Zr_8$ alloys) revealed that, contrary to the earlier finding,[2,3] the exponents β, γ, and δ (exponent for the critical isotherm) possess values which are fairly close to the 3D NN Heisenberg values. This result casts serious doubts about the genuineness of the anomalously large critical exponent values reported[3] for *a*-$Fe_{90-x}(Co,Ni)_xZr_{10}$ alloys and hence necessitates a detailed study of the critical behavior in these alloys. In this paper we describe an experimental determination of the exponents β and γ, which characterize the FM-PM phase transition at T_C, the Curie temperature, for the *a*-$Fe_{90-x}Co_xZr_{10}$ alloys. Although the ferromagnetic-resonance (FMR) technique as such is old and the related technique called the "zero"-applied-field ferromagnetic-antiresonance (FMAR) microwave transmission technique has been successfully used[7] in the past to determine the exponent β for crystalline Fe and Ni, we demonstrate that the FMR technique can yield accurate estimates of the exponents β and γ for ferromagnets through a detailed comparative study on the *a*-$Fe_{90}Zr_{10}$ alloy which involves bulk magnetization and FMR measurements performed on the same sample in the critical region.

II. EXPERIMENTAL DETAILS

Amorphous $Fe_{90-x}Co_xZr_{10}$ alloys with $x=0$, 1, 2, 4, 6, and 8 were prepared under argon (inert) atmosphere by the single-roller melt-quenching technique in the form of $\sim$2-mm-wide and (20–30)-μm-thick ribbons. The amorphous state of the ribbons was confirmed by x-ray-diffraction and electron microscopic methods. Using a PAR 4500 vibrating-sample magnetometer, magnetization (M) versus external magnetic-field (H_{ex}) isotherms were measured at 0.1-K intervals in the critical region on several 6-mm-long strips of the *a*-$Fe_{90}Zr_{10}$ alloy stacked one above the other in fields upto 15 kOe directed along the length in the ribbon plane so as to minimize the demagnetization effects. The sample temperature was held constant to within ±25 mK by a Lakeshore DRC 93C temperature controller and monitored by a precalibrated copper-constantan thermocouple in contact with the sample. The microwave power (P) absorption derivative dP/dH for *a*-$Fe_{90-x}Co_xZr_{10}$ alloys with $x=0$, 1, 2, 4, 6, and 8 was measured as a function of the external static magnetic field (H) on 4-mm-long strips, cut from the alloy ribbons, using horizontal-parallel ($\|^h$) and vertical-parallel ($\|^v$) sample configurations (in which H

lies in the ribbon plane and is directed along the length and breadth, respectively) at a fixed microwave-field frequency of ~9.225 GHz on a JEOL FE-3X EPR spectrometer in the temperature range $-0.1 \lesssim \varepsilon = (T - T_C)/T_C \lesssim 0.1$ at 0.5-K intervals. A copper-constantan thermocouple situated just outside the microwave cavity a few centimeters away from the sample was used as a temperature-controlling sensor, and the temperature T^* at the location of this sensor was held constant to within ± 0.1 K at every temperature setting by regulating the flow of cold nitrogen gas around the sample, mounted in a stress-free condition[8] inside a quartz tube, by controlling the power input to the heater, immersed in a container filled with liquid nitrogen, with the aid of a proportional, integral, and derivative (PID) temperature controller. The sample temperature T_s in this case also was measured by means of a precalibrated copper-constantan thermocouple and was found to be stable to within $T \pm 50$ mK when T^* fluctuates between $T - 0.1$ and $T + 0.1$ K at a given temperature T. No change in T_s due to eddy currents was detected when the microwave power level is increased from zero to 1 mW. Note that $P = 1$ mW for all the measured dP/dH-vs-H isotherms and that the FMR and BM measurements were performed on the *same* a-$Fe_{90}Zr_{10}$ sample. Based on a detailed compositional analysis and the observed dependence of T_C on Co concentration, we conclude that the rounding of the transition in zero field should occur for temperatures $\varepsilon \lesssim 4 \times 10^{-4}$. Thus the data taken in this temperature range are not included in the analysis. Repeated FMR experimental runs on the same sample have revealed that the resonance field H_{res} (defined as the field where the $dP/dH = 0$ line cuts the dP/dH-vs-H curve) and "peak-to-peak" linewidth ΔH_{pp} are reproduced to within $\pm 1\%$ and $\pm 10\%$, respectively.

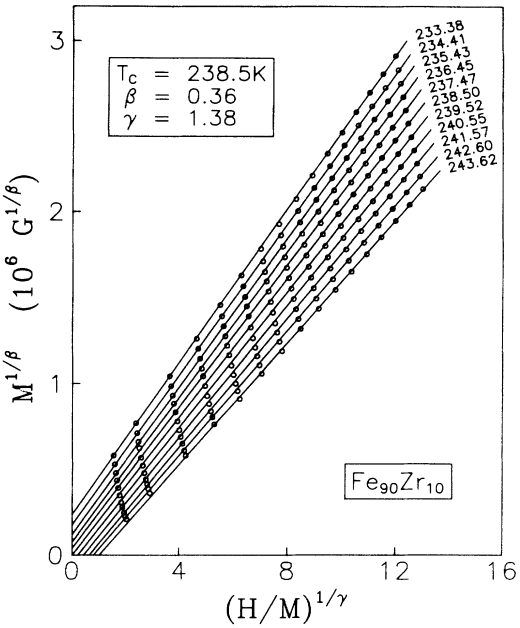

FIG. 1. Modified Arrott plot constructed using the bulk magnetization data taken on the a-$Fe_{90}Zr_{10}$ alloy.

III. EXPERIMENTAL RESULTS: DATA ANALYSIS AND DISCUSSION

A. Bulk magnetization

Figure 1 displays the M-vs-H_{ex} isotherms taken on the amorphous (a-) $Fe_{90}Zr_{10}$ alloy in a narrow temperature range around Curie point T_C in the form of a *modified* Arrott plot [i.e., $M^{1/\beta}$ vs $(H/M)^{1/\gamma}$]. The values of the exponents β and γ used to construct this plot and given

TABLE I. Values for the parameters that characterize the critical behavior near the FM-PM phase transition in amorphous $Fe_{90-x}Co_xZr_{10}$ alloys and a comparison between the experimentally determined and theoretically predicted values for the critical exponents β and γ and for the universal critical amplitude ratio $\mu_0 h_0/k_B T_C$. The number in the parentheses denotes the uncertainty in the least significant figure, and (1), (2), and (3) denote the first, second, and third experimental runs on the same sample. BM stands for bulk magnetization, whereas FMR is the abbreviation for ferromagnetic resonance.

Alloy concentration (x)/theory	Method	T_C (K)	β	γ	m_0 (G)	h_0/m_0	h_0 (10^5 G)	$\mu_0(\mu_B)$[a]	$\mu_0 h_0/k_B T_C$	$\mu_{eff}(\mu_B)$	c (%)
0	FMR (1)	238.55(15)	0.380(30)	1.40(6)	870(30)	500(50)	4.4(6)	1.386	0.172(17)	12.7(16)	11.0(10)
	FMR (2)	238.50(15)	0.370(30)	1.39(6)	870(30)	525(50)	4.6(6)	1.386	0.180(20)	12.2(17)	11.0(11)
	FMR (3)	238.55(15)	0.380(30)	1.38(6)	865(30)	500(50)	4.3(6)	1.386	0.168(17)	13.0(15)	11.0(10)
	BM	238.50(5)	0.360(20)	1.38(3)	870(25)	500(50)	4.4(6)	1.386	0.172(16)	12.7(16)	11.0(10)
1	FMR (1)	254.50(20)	0.380(30)	1.38(6)	1030(35)	500(75)	5.1(9)	1.50	0.202(35)	11.7(18)	12.8(15)
	FMR (2)	254.80(20)	0.380(30)	1.38(6)	1045(25)	430(50)	4.5(7)	1.50	0.178(22)	13.3(15)	11.3(10)
2	FMR (1)	284.00(25)	0.375(25)	1.38(5)	1070(25)	400(60)	4.3(8)	1.61	0.164(30)	11.3(10)	10.4(16)
	FMR (2)	284.50(25)	0.385(25)	1.38(5)	1065(25)	450(50)	4.8(6)	1.61	0.182(22)	13.9(15)	11.6(10)
4	FMR (1)	336.00(10)	0.386(20)	1.38(5)	1075(20)	650(50)	7.0(6)	1.68	0.235(16)	11.3(10)	15.0(12)
	FMR (2)	335.85(10)	0.380(20)	1.39(6)	1075(20)	650(50)	7.0(6)	1.68	0.235(16)	11.3(10)	15.0(12)
6	FMR (1)	377.04(10)	0.375(25)	1.38(5)	1160(30)	950(50)	11.0(9)	1.70	0.333(25)	8.0(6)	21.5(15)
	FMR (2)	377.10(10)	0.385(25)	1.39(6)	1165(30)	950(50)	11.0(8)	1.70	0.333(25)	8.0(6)	21.2(15)
8	FMR (1)	419.50(10)	0.384(20)	1.38(6)	1215(35)	1200(50)	14.6(7)	1.70	0.397(18)	6.8(5)	25.0(18)
	FMR (2)	419.55(10)	0.382(20)	1.38(6)	1215(35)	1200(50)	14.6(7)	1.70	0.397(18)	6.8(5)	25.0(18)
3D Heisenberg			0.365(3)	1.386(4)					1.58		

[a]Values obtained from the bulk magnetization measurements taken at 4.2 K on the glassy alloys under consideration.

in Table I have been determined by the *modified* asymptotic analysis (AA-II; for details see Ref. 9), and the magnetic field H has been corrected for the demagnetizing effects (i.e., $H=H_{ex}-H_{dem}$, where H_{dem} is the demagnetizing field estimated from the "low-field" magnetization data). The isotherms are seen to be a set of straight lines, and the critical isotherm at $T=T_C=238.50$ K passes through the origin, as expected for a correct choice of the exponents β and γ.

B. Ferromagnetic resonance

The variation of dP/dH with H in the $\|^h$ configuration at a few selected values of temperature in the critical region is depicted for a-$Fe_{90}Zr_{10}$ in Fig. 2. These curves are also representative of those recorded for a-$Fe_{90}Zr_{10}$ in the $\|^v$ configuration and for other alloys in both $\|^h$ and $\|^v$ geometries. It is evident from Fig. 2 that as the temperature is increased through T_C, the peak in the dP/dH-vs-H curves at a lower field value ~ 800 Oe develops into a full-fledged resonance (secondary resonance) for $T \gtrsim T_C+10$ K, whereas the main (primary) resonance shifts to higher fields and broadens out. A detailed FMR study[10] carried out on the glassy alloys in question in a wide temperature range $77 \leq T \lesssim 500$ K reveals that the secondary-resonance (whose signature is first noticed in the most sensitive setting of the spectrometer at a temperature close to T_C or above T_C) exhibits a "cluster spin-glass-like" behavior, whereas the primary resonance possesses properties *characteristic* of ferromagnets with[11,12] (for $x \lesssim 2$) or without[12] (for $x \gtrsim 2$) reentrant spin-glass behavior at low temperatures. Since the study of critical behavior near the FM-PM phase transition in a-$Fe_{90-x}Co_xZr_{10}$ alloys is of prime concern in this paper and the data recorded in $\|^h$ and $\|^v$ configurations yield exactly the same results so far as the critical behavior in the investigated glassy alloys is concerned, henceforth we deal with the primary resonance part of the dP/dH-vs-H curves, recorded in the $\|^h$ configuration, only. Now that in the critical region $\Delta H_{pp} \cong H_{res}/4$, the observed value of H_{res} could significantly differ from the "true" resonance center, and hence a detailed line-shape analysis for each resonance line separately is called for. The dP/dH-vs-H curves recorded at different temperatures in the $\|^h$ configuration have been fitted to the theoretical expression[10,13]

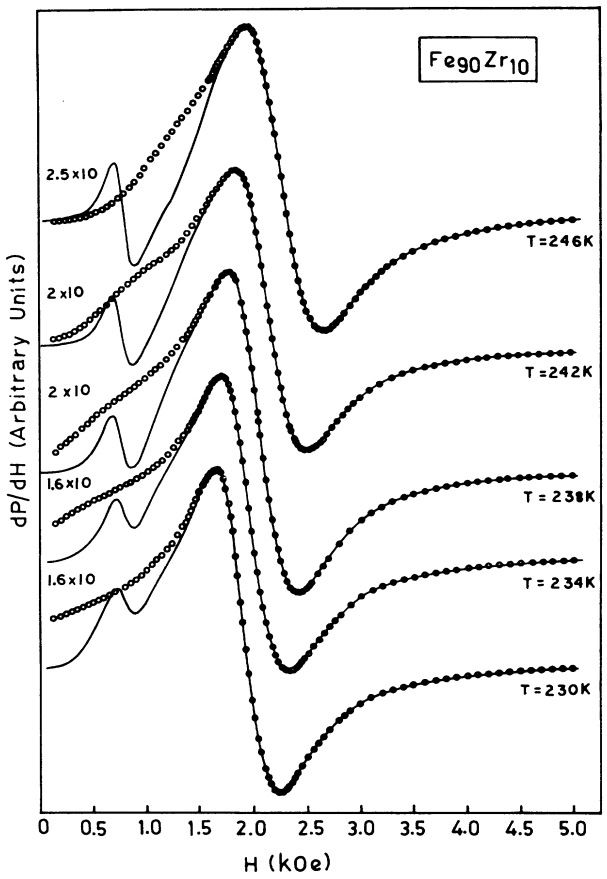

FIG. 2. Power absorption derivative curves for a-$Fe_{90}Zr_{10}$ at a few representative temperature values in the critical region recorded using the $\|^h$ sample configuration. Solid curves depict the observed variation of dP/dH with H, whereas the open circles denote the calculated values based on Eqs. (1) and (2) of the text. Numbers on the left-hand side of the curves are a measure of the sensitivity at which the spectra are taken.

$$\frac{dP_{\|}}{dH} \propto \frac{d}{dH}[(\mu'^2+\mu''^2)^{1/2}+\mu'']^{1/2}, \tag{1}$$

with the real and imaginary components of the dynamic permeability given by

$$\mu'=\frac{[(H+H_K)(B+H_K)-\Gamma^2-(\omega/\gamma)^2][(B+H_K)^2-\Gamma^2-(\omega/\gamma)^2]+2\Gamma^2(B+H_K)(B+H+2H_K)}{[(H+H_K)(B+H_K)-\Gamma^2-(\omega/\gamma)^2]^2+\Gamma^2(B+H+2H_K)^2} \tag{2a}$$

and

$$\mu''=\frac{-2\Gamma(B+H_K)[(H+H_K)(B+H_K)-\Gamma^2-(\omega/\gamma)^2]+\Gamma(B+H+2H_K)[(B+H_K)^2-\Gamma^2-(\omega/\gamma)^2]}{[(H+H_K)(B+H_K)-\Gamma^2-(\omega/\gamma)^2]^2+\Gamma^2(B+H+2H_K)^2} \tag{2b}$$

derived for dP/dH in the parallel geometry and obtained by solving the Landau-Lifshitz-Gilbert (LLG) equation of motion in conjunction with Maxwell's equations, by making use of a nonlinear least-squares-fit computer program which treats the Landé splitting factor g and saturation magnetization $M_s=(B-H)/4\pi$ as free fitting parameters and uses the observed values of $\Delta H_{pp}=1.45\Gamma=1.45\lambda\omega/\gamma^2 M_s$ (where λ is the Gilbert

damping parameter, $\gamma = g|e|/2mc$, and $\nu = \omega/2\pi$ is the microwave-field frequency), and values of the "in-plane" uniaxial anisotropy field H_K deduced from the relations[10]

$$H_{\text{res}}^{\parallel^h} = H_{\text{res}}^{\parallel} - H_K \tag{3a}$$

and

$$H_{\text{res}}^{\parallel^v} = H_{\text{res}}^{\parallel} + H_K \ . \tag{3b}$$

In Eqs. (3a) and (3b), $H_{\text{res}}^{\parallel^h}$ and $H_{\text{res}}^{\parallel^v}$ are the estimates for the resonance fields in the $\parallel^h$ and $\parallel^v$ configurations, respectively, obtained after correcting the observed values for the demagnetization fields $H_{\text{dem}}^{\parallel^h}$ and $H_{\text{dem}}^{\parallel^v}$, determined from the low-field magnetization measurements performed on the samples used for the present FMR study with the external magnetic field applied along the easy ($\parallel^h$-configuration) and hard ($\parallel^v$-configuration) directions in the ribbon plane, and $H_{\text{res}}^{\parallel}$ is the resonance field in the absence of H_K. In the line-shape calculations leading to Eqs. (1), (2a), and (2b), the exchange-conductivity contribution has been dropped in view of the well-known observation[10,14,15] that this contribution to the linewidth as well as to the resonance field is so small as to fall well within the error limits because the values for the exchange stiffness parameter and conductivity both are at least an order of magnitude smaller[16,17] than their corresponding values for crystalline metals.

Theoretical fits, depicted by open circles in Fig. 2, not only assert that the line-shape analysis yields "true" values of the line centers for the primary resonance even in the presence of a secondary resonance because the baseline for the two resonances is the *same* (Fig. 2), but also indicate that the LLG equation adequately describes the resonant behavior in the critical region. In addition, the line-shape calculations reveal that the splitting factor g has a constant value of 2.07 ± 0.02 within the investigated temperature range. That the g factor is temperature independent and the LLG equation forms an adequate description of $H_{\text{res}}(T)$ and $\Delta H_{\text{pp}}(T)$ in the critical region for crystalline ferromagnets also has been claimed by Rodbell[18] and by Haraldson and Pettersson,[19] but this claim has been refuted by Bhagat and Rothstein.[20] The present results are, however, consistent with our earlier observation[10] that $M_s(T)$ deduced in this way[21] from the FMR data are in excellent agreement with $M(T)$ measured on the same sample at an external magnetic field whose strength is comparable to H_{res}.

C. Critical exponents, amplitudes, and scaling equation of state

Having determined $M_s(T)$ and $H_{\text{res}}(T)$ [$\equiv H_{\text{res}}^{\parallel^h}(T)$; the superscript $\parallel^h$ is henceforth dropped for convenience] to a high precision from the line-shape calculations, accurate values of β, γ, and T_C are extracted from the $M(H,T) \equiv M_s(H_{\text{res}},T)$ data by identifying H_{res} with the ordering field H conjugate to M ($\equiv M_s$), and using the "range-of-fit" scaling-equation-of-state (SES) analysis,[22] which is based on the magnetic equation of state,

$$m = f_{\pm}(h) \ , \tag{4}$$

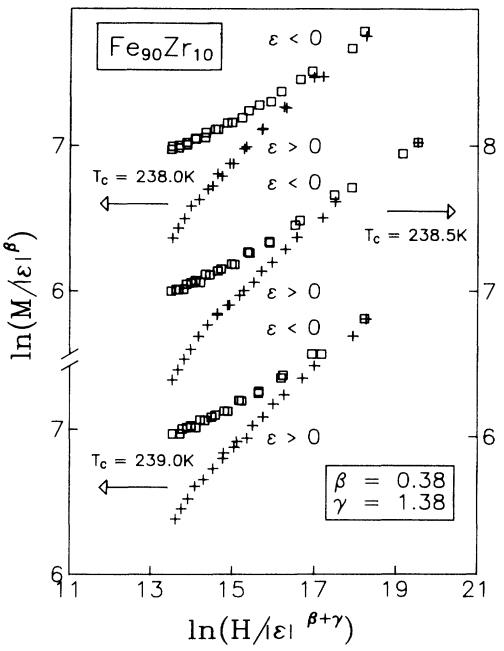

FIG. 3. Plots of $\ln(M/|\varepsilon|^{\beta})$ against $\ln(H/|\varepsilon|^{\beta+\gamma})$ for different values of T_C for a-$Fe_{90}Zr_{10}$.

where plus and minus signs refer to temperatures above and below T_C and $m \equiv M/|\varepsilon|^{\beta}$ and $h \equiv H/|\varepsilon|^{\beta+\gamma}$ are the scaled magnetization and scaled field, respectively. In the conventional SES method,[9] $M(H,T)$ data, in the critical region, are made to fall on two universal curves, f_- for $\varepsilon < 0$ and f_+ for $\varepsilon > 0$, through an appropriate choice of the parameters T_C, β, and γ in an m-vs-h plot, but this choice is by no means unique in the sense that nearly the same quality of data collapse onto the two universal curves can be achieved for a wide range of parameter values (typically, $\pm 2\%$ for T_C and $\pm 10\%$ for β and γ). This problem is, however, effectively tackled by employing the range-of-fit SES analysis[22] in which more and more of the data taken at temperatures away from T_C are excluded from the m-vs-h plot so that the exponents β and γ become increasingly sensitive to the choice of T_C and the data exhibit strong departures from the curves $f_-(h)$ and $f_+(h)$ if the choice of the parameters differs even slightly from the correct one. This procedure, therefore, goes on refining the values of the critical exponents until they approach the *asymptotic* values. The final values of the parameters T_C, β, and γ for a-$Fe_{90}Zr_{10}$ so obtained are given in Table I. Figure 3 serves to illustrate the effect of the variation in the value of T_C on the quality of data collapse. Similar effects are observed if one of the exponents is varied while keeping T_C and the other exponent fixed.

A comparison between the $\ln m$-vs-$\ln h$ scaling plots for a-$Fe_{90}Zr_{10}$ constructed using the BM and FMR data (recorded in three different experimental runs) taken on the same sample is shown in Fig. 4. A perfect agreement between different sets of FMR data and between the results of FMR and BM measurements is evident from this figure. However, a more rigorous means[9] of ascertaining

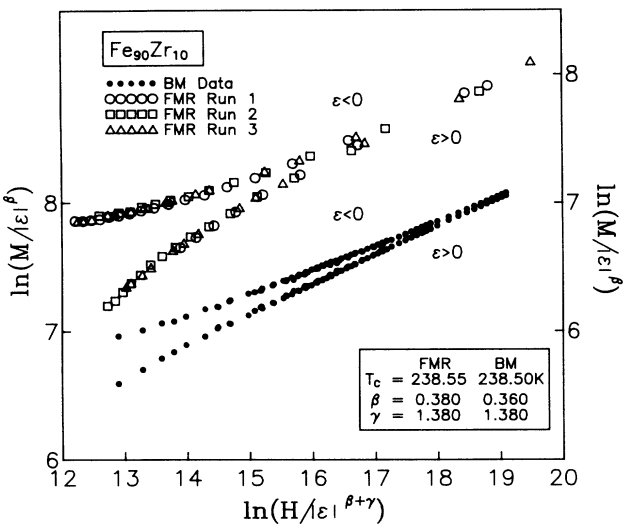

FIG. 4. $\ln(M/|\varepsilon|^{\beta})$-vs-$\ln(H/|\varepsilon|^{\beta+\gamma})$ plots for a-$Fe_{90}Zr_{10}$ constructed using the bulk magnetization data and saturation magnetization data deduced from FMR spectra employing lineshape analysis.

whether or not the above method yields accurate values for the critical exponents and T_C is provided by a SES form that differs from Eq. (4), i.e.,

$$m^2 = \mp a_{\pm} + b_{\pm}(h/m) \tag{5}$$

(where the plus and minus signs as well as m and h have the same meaning as given above), because even the slightest deviations of the data from the universal curves $f_-(h)$ and $f_+(h)$, which do not show up clearly in a $\ln m$-vs-$\ln h$ plot because of the insensitive nature of the double-logarithmic scale, become easily discernible[23] when the same data are plotted in the form of an m^2-vs-(h/m) plot. Another advantage in using Eq. (5) is that the critical amplitudes $m_0 = a_-^{1/2}$ and $h_0/m_0 = a_+/b_+$, defined by

$$M_s(\varepsilon) = \lim_{H\to 0} M(H,\varepsilon) = m_0(-\varepsilon)^{\beta}, \quad \varepsilon < 0 \tag{6a}$$

and

$$\chi_0^{-1}(\varepsilon) = \left[\left|\frac{\partial M(H,\varepsilon)}{\partial H}\right|_{H=0}\right]^{-1} = (h_0/m_0)\varepsilon^{\gamma}, \quad \varepsilon > 0 \tag{6b}$$

are given by the intercepts of the universal curves with m^2 and h/m axes, respectively, in an m^2-vs-h/m plot. Such plots constructed using the choice of parameters T_C, β, and γ given in Table I are shown in Figs. 5(a) and 5(b). Consistency among different sets of data is now all the more obvious, particularly when the BM and FMR data are plotted on a highly sensitive scale and only those BM data that are taken at fields comparable in strength to those used in FMR experiments are included in Fig. 5(a). From the observation that no deviations from the universal curves are evident even at low fields in Figs. 5(a) and 5(b), we conclude that the values for the critical exponents and T_C determined by the range-of-fit SES analysis are reasonably accurate. Moreover, the value of the specific-heat critical exponent $\alpha = -0.14$, computed using the presently determined values of the exponents β and γ (which conform very well with those previously reported[1,5] for this alloy based on the BM measurements) in the scaling relation $\alpha = 2(1-\beta)-\gamma$, and the present value of T_C (Table I) agree closely with those ($\alpha = -0.13 \pm 0.06$, $T_C = 238.6 \pm 0.1$ K) extracted from recent electrical resistivity measurements[17] on a sample cut from the same a-$Fe_{90}Zr_{10}$ ribbon as that used in this work. Table I lists the values of Curie temperature, critical exponents β and γ, critical amplitudes m_0 and (h_0/m_0), and the ratio $\mu_0 h_0/k_B T_C$, deduced for the a-$Fe_{90}Zr_{10}$ alloy from the BM data and from the different sets of FMR data taken on the same sample, and com-

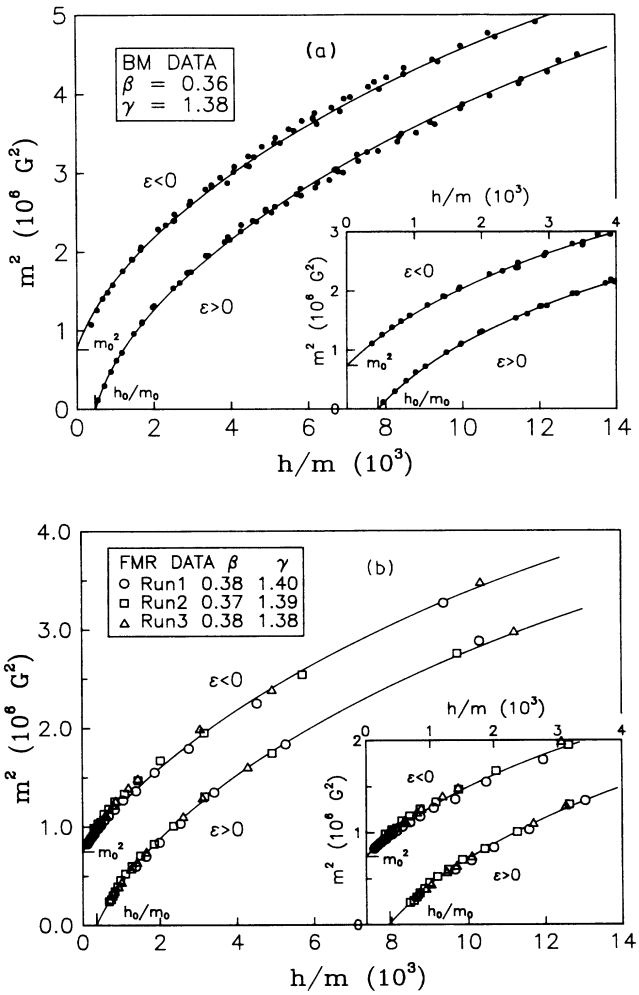

FIG. 5. m^2-vs-h/m plot for a-$Fe_{90-x}Zr_{10}$ constructed using (a) bulk magnetization data and (b) saturation magnetization data deduced from the FMR spectra taken in the first (open circles), second (open squares), and third (open triangles) experimental runs on the same sample. The data near the origin are plotted on a sensitive scale in the inset with a view to bring out values of the intercepts m_0^2 and h_0/m_0 on m^2 and h/m axes clearly.

pares them with the theoretical values predicted for an isotropic NN 3D Heisenberg ferromagnet. An assessment of the data presented in Table I reveals that a remarkably close agreement exists not only between the BM and FMR results, but also between the theoretical and experimental values for the critical exponents. However, the observed value of the ratio $\mu_0 h_0/k_B T_C$ is one order of magnitude smaller than the theoretically predicted one. Since h_0 is presumably an *effective* exchange interaction field, the product of h_0 and an *average effective* elementary moment (μ_{eff}) involved in the FM-PM phase transition, i.e., the effective exchange energy $\mu_{\text{eff}} h_0$, is expected to equal the thermal energy $k_B T_C$ at T_C. Obviously, this is not the case for a-$Fe_{90}Zr_{10}$ unless μ_{eff} is taken to be very much larger than μ_0 (average magnetic moment per alloy atom at 0 K). Now that the exponents possess 3D Heisenberg values, the ratio $\mu_{\text{eff}} h_0/k_B T_C$ is also expected to equal the 3D Heisenberg estimate of 1.58. This is possible only when μ_{eff} assumes the values given in Table I. Moreover, if the concentration of such effective moments is c, then $c = \mu_0/\mu_{\text{eff}}$. The values of c calculated in this way and included in the Table I strongly indicate that only a small fraction of moments (i.e., the moments on Fe atoms in the case of a-$Fe_{90}Zr_{10}$) participates in the FM-PM phase transition.

Having demonstrated that the FMR technique is a powerful tool for investigating the critical behavior in ferromagnets, accurate values for T_C, the critical exponents β and γ, critical amplitudes m_0 and (h_0/m_0), and concentration of effective moments participating in the FM-PM transition, c, have been determined by analyzing the FMR data taken on the alloys with $x = 1$, 2, 4, 6, and 8 using the same method as mentioned above. The values so obtained are listed in Table I and are used to construct the m^2-vs-h/m scaling plots for the Co-containing glassy alloys shown in Fig. 6. A number of interesting points emerge from a comparison of the present

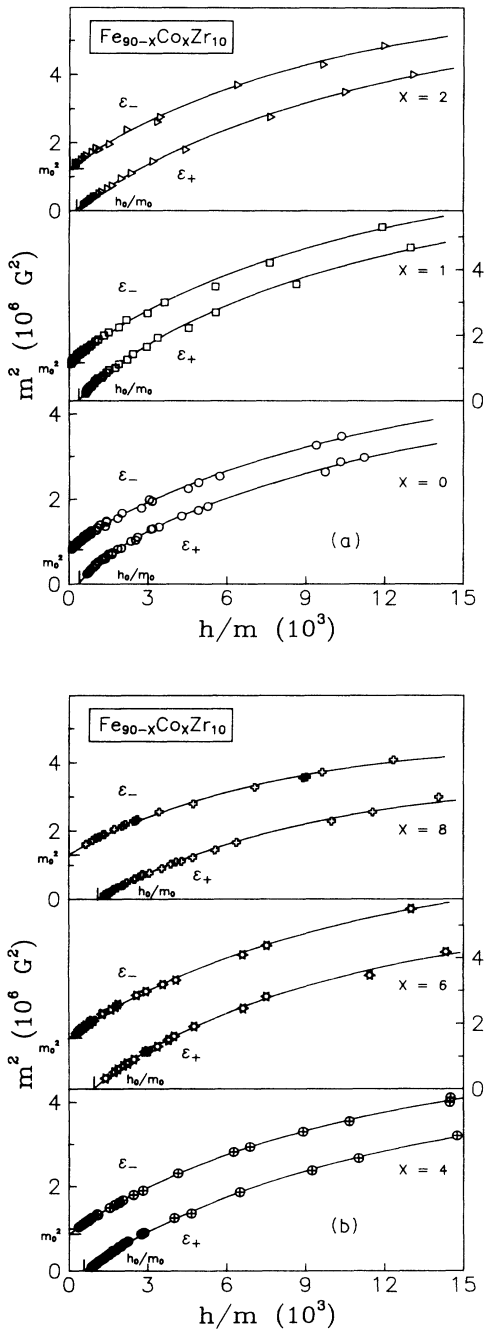

FIG. 6. m^2-vs-h/m plots for a-$Fe_{90-x}Co_xZr_{10}$ alloys constructed using the saturation magnetization data deduced from the FMR spectra recorded at different temperatures in the critical region.

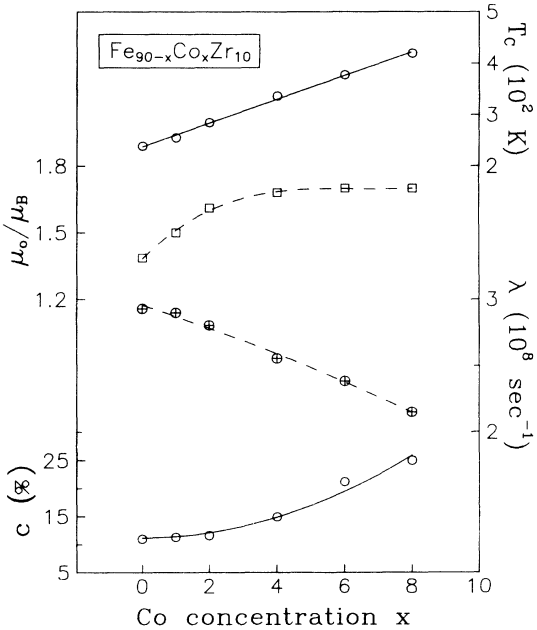

FIG. 7. Functional dependences of Curie temperature T_C, magnetic moment per alloy atom at 0 K, μ_0, Gilbert damping parameter λ, and the fraction of spins participating in the FM-PM phase transition, c, on the Co concentration x for a-$Fe_{90-x}Co_xZr_{10}$ alloys. The solid curves are the least-squares fits to the data, whereas the dashed curves serve as a guide to the eye. Note that the error limits for λ are typically $\pm 5\%$ of its value at a given x. The error limits for the other quantities are given in Table I.

results with those previously[3] obtained and with those predicted by the theory;[4] namely, (i) contrary to the earlier finding,[3] the exponents β and γ *do not depend* on the alloy composition and possess 3D-Heisenberg-like values; (ii) the fraction of spins that actually participates in the FM-PM phase transition, c, is small for the parent alloy ($x=0$), but increases with Co concentration x as $c(x)-c(0)\cong ax^2$, with $c(0)=11\pm1\%$ and $a\cong0.23$, in the investigated composition range (Fig. 7); and (iii) in conformity with the previously reported[12] result, the Curie temperature T_C increases roughly linearly with the composition x [i.e., $T_C(x)=T_C(0)+23.2x$, with $T_C(0)=237.2$ K], whereas the moment per alloy atom at 0 K, μ_0, increases steeply with x in the range $0\lesssim x\lesssim2$ and attains saturation for $x\gtrsim4$ (Fig. 7).

D. FMR linewidth

Variation of the peak-to-peak FMR linewidth ΔH_{pp} with temperature is displayed in Fig. 8. A slope change in $\Delta H_{pp}(T)$ at T_C ($\varepsilon=0$) for all the glassy alloys under consideration is indicative of a well-defined magnetic phase transition at T_C. It should be emphasized at this stage that the values of ΔH_{pp} are the *same* (within error limits) for both $\|^h$ and $\|^v$ configurations at all temperatures within the temperature range covered in the present experiments. Hence $\Delta H_{pp}(T)$ observed in the $\|^h$ configuration and depicted in Fig. 8 reproduces all the features $\Delta H_{pp}^{\|^v}(T)$ even to the minutest detail. FMR measurements carried out, in the past, over a wide range of microwave-field frequencies at constant temperature ($T<T_C$) on a large number of amorphous ferromagnetic alloy systems have revealed[24–29] that the two main contributions[30] to ΔH_{pp} are ΔH_I, which is nearly independent of the microwave-field frequency $\nu=\omega/2\pi$ and is most probably caused by the two-magnon scattering from spatially localized magnetization inhomogeneities,[14,31,32] and $\Delta H_{LLG}=1.45\lambda\omega/\gamma^2M_s$, which has a linear dependence on ν and results from a LLG relaxation mechanism. In such materials, ΔH_{pp} is found to remain practically constant[9,10,14,15,24–29] over a wide range of temperatures well below T_C ($T\lesssim0.8T_C$) and the Gilbert damping parameter λ varies linearly[10,14,15,24–29] with M_s. An immediate consequence of the result $\lambda\propto M_s$ is that ΔH_{LLG} does not vary with temperature, so that in view of a constant value of ΔH_{pp} even ΔH_I should *not depend* on temperature. In the critical region ($-0.05\lesssim\varepsilon\lesssim0.05$), $\Delta H_{pp}(T)$ for all the amorphous alloys in question, with the exception of those with $x=0$ and 4, can be very well described (Fig. 9) by the empirical expression

$$\Delta H_{pp}(T)=\Delta H(0)+[A/M_S(T)]\ . \tag{7}$$

If the first and second terms on the right-hand side of Eq. (7) are identified with ΔH_I and ΔH_{LLG}, respectively, the coefficient A in Eq. (7), determined by the least-squares method for different compositions, permits a straightforward calculation of the damping parameter λ. Note that Eq. (7) with the meaning of the terms $\Delta H(0)$ and $A/M_s(T)$ same as above has been previously[27] used to

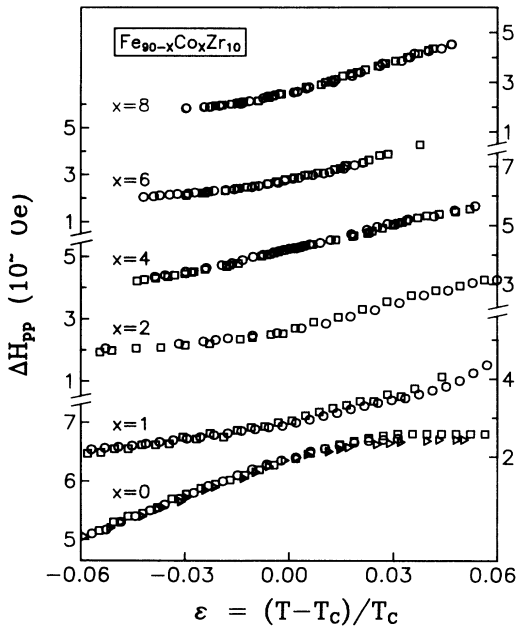

FIG. 8. Variation of the peak-to-peak FMR linewidth (ΔH_{pp}) with temperature in the critical region for *a*-$Fe_{90-x}Co_xZr_{10}$ alloys. The $\Delta H_{pp}(T)$ data taken in the first, second, and third experimental runs on the same sample are depicted by the symbols open circles, squares, and triangles, respectively.

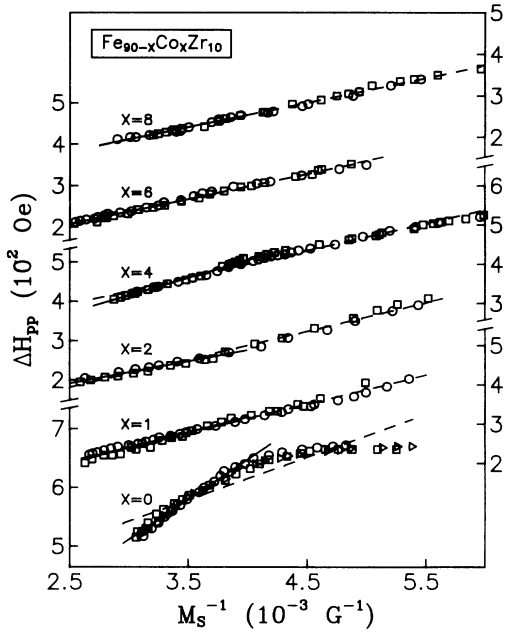

FIG. 9. Peak-to-peak FMR linewidth (ΔH_{pp}) plotted against inverse saturation magnetization in the temperature interval $-0.05\lesssim\varepsilon\lesssim0.05$ for $Fe_{90-x}Co_xZr_{10}$ alloys. The solid and dashed straight lines drawn through the data points (denoted by the symbols which have the same meaning as in Fig. 8) represent the least-squares fit to the $\Delta H_{pp}(T)$ data based on Eq. (7) of the text in the temperature intervals $-0.05\lesssim\varepsilon\lesssim0$ and $-0.05\lesssim\varepsilon\lesssim0.05$, respectively.

describe the temperature dependence of ΔH_{pp} in Fe-rich a-$Fe_{100-x}B_x$ alloys for temperatures well below T_C. *The temperature-independent* values of λ so computed range between 2×10^8 and 3×10^8 sec^{-1} and exhibit a *weak decreasing* trend with Co concentration as shown in Fig. 7. By contrast, the intercept $\Delta H(0)$ does not show any systematic trend with x; i.e., a minimum [$\Delta H_{min}(0)\cong20$ Oe] in the $\Delta H(0)$-vs-x curve at $x=2$ is followed by a maximum [$\Delta H_{max}(0)\cong140$ Oe] at $x=4$. Different sets of FMR data taken on the same sample demonstrate that the values for λ are reproduced to within $\pm10\%$. Another important finding which merits attention is that the quality of the least-squares fits to the $\Delta H_{pp}(T)$ data based on Eq. (7) improves, as inferred by a lower value for the sum of deviation squares (χ^2), if the range of temperatures over which such fits are attempted is confined to temperatures just below T_C, i.e., $0.05\lesssim\varepsilon\lesssim0$. However, a marked improvement in the quality of these fits, brought about by a widely different choice of the parameters $\Delta H(0)$ and A [i.e., $\Delta H(0)$ decreases by a factor of about 1.5, while A (and hence λ) increases by the same factor] is observed for the alloys with $x=0$ and 4 only; for the remaining alloys, the slope and intercept values change only slightly from their previous estimates, with the result that only a marginal decrease in χ^2 occurs. The appearance of the secondary resonance at $T\cong T_C$ for a-$Fe_{90}Zr_{10}$ and at a temperature a few degrees above T_C for the alloy with $x=4$ as against at temperatures well above T_C for other alloys could be at the root of the unique behavior of the alloys with $x=0$ and 4. A complete understanding of this aspect of the FMR data must, however, await a detailed investigation which sheds light on the exact origin of the secondary resonance. The presently determined values of the damping parameter λ are about 3 times larger than those reported for a wide variety of crystalline[18,19,33,34] and amorphous[24–29,35] ferromagnets at temperatures well below the Curie temperature T_C. Such a *large enhancement* in the value of λ for temperatures close to T_C is not uncommon.[19,36] Moreover, the finding that λ *does not depend* on temperature in the critical region is a property which the investigated glassy alloys share with crystalline ferromagnets;[18,19,37,38] detailed but accurate measurements of $\Delta H_{pp}(T)$ in the critical region for amorphous ferromagnets are presently lacking.

Considering the well-known[15,27] fact that the dynamic permeability attains its maximum value at the field corresponding to ferromagnetic resonance and the microwave radiation penetrates only a thin surface layer (typically[15,27] 10^3 Å) in a ferromagnetic metal, FMR measurements have also been performed on the BM samples after etching them with nital (10% concentrated HNO_3 + 90% C_2H_5OH) solution for 30 min so as to ensure that the results are representative of the bulk. From the weight-loss measurements, we infer that the thickness of the sample is reduced to nearly half after the etching treatment. Apart from a systematic downward shift (upward shift) in the resonance field (saturation magnetization) versus temperature curve for the etched samples with respect to the similar curve in the "as-quenched" samples, no change in the values quoted for different quantities in Table I has been detected. It should be emphasized at this stage that the full potential of the FMR technique to yield accurate values for the critical exponents can be exploited only when this technique is used to study the magnetic order-disorder phase transition in good quality thin films since the skin depth in that case is comparable to the film thickness and the conventional methods to measure bulk magnetization for samples in thin-film form lack the required sensitivity.

IV. CONCLUSION

From a detailed study of critical behavior in amorphous $Fe_{90-x}Co_xZr_{10}$ alloys using bulk magnetization (for the alloy with $x=0$ alone) and FMR techniques, the following conclusions can be drawn.

(i) The FMR technique can be used to determine the critical exponents β and γ for ferromagnets to an accuracy which compares well with that achieved in the bulk magnetization method.

(ii) Contrary to the earlier claim,[3] the critical exponents β and γ are *composition independent* and possess values which are close to the renormalization-group estimates for a spin system with spin as well as spatial dimensionality of three. Alternatively, the transition at T_C is well defined and the quenched disorder does not alter the critical behavior of an ordered 3D Heisenberg ferromagnet; i.e., the well-known Harris criterion is satisfied.

(iii) The fraction of spins that actually participates in the FM-PM phase transition, c, increases from 11% at $x=0$ to 25% at $x=8$ and the functional dependence of c on x is well described by the empirical relation $c(x)-c(0)\cong ax^2$.

(iv) $\Delta H_{pp}(T)$ closely follows a relation of the type $\Delta H_{pp}(T)=\Delta H(0)+[A/M_s(T)]$ in the critical region.

(v) Both the Landé splitting factor g and Gilbert damping parameter λ are *temperature independent* within the investigated temperature range, but with increasing Co concentration λ decreases while g remains constant at the value 2.07 ± 0.02.

ACKNOWLEDGMENTS

The financial support by the Department of Science and Technology, New Delhi, under project No. SP/S2/M21/86 to carry out this work is gratefully acknowledged. One of us (P.D.B.) is thankful to the University Grants Commission, New Delhi, for financial assistance.

[1]S. N. Kaul, J. Phys. F **18**, 2089 (1988).
[2]H. Yamauchi, H. Onodera, and H. Yamamoto, J. Phys. Soc. Jpn. **53**, 747 (1984).
[3]K. Winschuh and M. Rosenberg, J. Appl. Phys. **61**, 4401 (1987).
[4]L. C. Le Guillou and J. Zinn-Justin, Phys. Rev. B **21**, 3976 (1980).
[5]R. Reisser, M. Fähnle, and H. Kromüller, J. Magn. Magn. Mater. **75**, 45 (1988).
[6]H. Hiroyoshi, K. Fukamichi, A. Hoshi, and Y. Nakagawa, in *High Field Magnetism,* edited by M. Date (North-Holland, Amsterdam, 1983), p. 113.
[7]J. D. Cohen and T. R. Carver, Phys. Rev. B **15**, 5350 (1977); J. H. Abeles, T. R. Carver, and G. C. Alexandrakis, J. Appl. Phys. **53**, 7935 (1982).
[8]S. N. Kaul and T. V. S. M. Mohan Babu, J. Phys. Condens. Matter. **1**, 8509 (1989).
[9]S. N. Kaul, J. Magn. Magn. Mater. **53**, 5 (1985).
[10]S. N. Kaul and V. Siruguri, J. Phys. Condens. Matter. (to be published), and unpublished results.
[11]S. N. Kaul, Phys. Rev. B **27**, 6923 (1983).
[12]P. Deppe, K. Fukamichi, F. S. Li, M. Rosenberg, and M. Sostarich, IEEE Trans. Magn. **MAG-20**, 1367 (1984).
[13]S. N. Kaul and V. Siruguri, J. Phys. F **17**, L255 (1987).
[14]S. M. Bhagat, S. Haraldson, and O. Beckman, J. Phys. Chem. Solids **38**, 593 (1977).
[15]S. N. Kaul and V. Srinivasa Kasyapa, J. Mater. Sci. **24**, 3337 (1989).
[16]S. N. Kaul, J. Phys. Condens. Matter **3**, 4027 (1991).
[17]Ch. V. Mohan, P. D. Babu, M. Sambasiva Rao, T. Lucinski, and S. N. Kaul (unpublished).
[18]D. S. Rodbell, Phys. Rev. Lett. **13**, 471 (1964).
[19]S. Haraldson and L. Pettersson, J. Phys. Chem. Solids **42**, 681 (1981).
[20]S. M. Bhagat and M. S. Rothstein, Solid State Commun. **11**, 1535 (1972), and references cited therein.
[21]The customary approach of determining $M_s(T)$ either by using the resonance condition for the $\|^h$ configuration and the results of FMR measurements performed in the same configuration at three widely spaced values of microwave frequency ν or by making use of the resonance conditions for the $\|^h$ and $\perp^h$ (the horizontal-perpendicular sample geometry, in which the external static magnetic field is applied perpendicular to the sample plane) configurations and the FMR results obtained for these sample configurations at a single value of ν has not followed in this work for two reasons. First, the lack of experimental facilities required for such an experimental investigation. Second, even with utmost care exercised in sample mounting and its positioning in the external static field, the line shape for the $\perp^h$ configuration and hence the value of $H_{\rm res}^{\perp^h}$ could not be reproduced with as high an accuracy as was achieved in the determination of $H_{\rm res}^{\|^h}$ and $H_{\rm res}^{\|^v}$ presumbly because of the *extreme sensitivity* of $H_{\rm res}^{\perp^h}$ to the angle between the field direction and sample plane. In view of this observation, we consider a perfect agreement observed between the values of $H_{\rm res}^{\perp^h}$ extracted from some experimental runs and those calculated using the numerical estimates of g and M_s, deduced from the present line-shape analysis of the FMR spectra taken in the $\|$ configuration, in the resonance condition for the $\perp^h$ configuration, as *fortuitous.*
[22]M. Fähnle, W. U. Kellner, and H. Kronmüller, Phys. Rev. B **35**, 3640 (1987); W. U. Kellner, M. Fähnle, H. Kronmüller, and S. N. Kaul, Phys. Status Solidi B **144**, 397 (1987).
[23]S. N. Kaul, Phys. Rev. B **23**, 1205 (1981).
[24]M. L. Spano and S. M. Bhagat, J. Magn. Magn. Mater. **24**, 143 (1981).
[25]L. Kraus, Z. Frait, and J. Schneider, Phys. Status Solidi A **63**, 669 (1981).
[26]J. F. Cochran, K. Myrtle, and B. Heinrich, J. Appl. Phys. **53**, 2261 (1982).
[27]B. Heinrich, J. M. Rudd, K. Urguhart, K. Myrtle, J. F. Cochran, and R. Hasegawa, J. Appl. Phys. **55**, 1814 (1984).
[28]D. J. Webb and S. M. Bhagat, J. Magn. Magn. Mater. **42**, 109 (1984).
[29]S. M. Bhagat, D. J. Webb, and M. A. Manheimer, J. Magn. Magn. Mater. **53**, 209 (1985).
[30]An additional contribution to $\Delta H_{\rm pp}$, besides $\Delta H_{\rm LLG}$ and ΔH_I, originates from the skin-depth effect (which makes the magnetization induced by the microwave field nonuniform in the volume of the surface penetration layer), but this contribution for the investigated alloys turns out to be as small as $\cong 10$ Oe (Ref. 15). This value lies well within the observed error limits and hence need not be considered while discussing different contributions to $\Delta H_{\rm pp}$.
[31]B. Heinrich, J. F. Cochran, and R. Hasegawa, J. Appl. Phys. **57**, 3690 (1985).
[32]J. F. Cochran, R. W. Qiao, and B. Heinrich, Phys. Rev. B **39**, 4399 (1989).
[33]S. M. Bhagat, in *Measurement of Physical Properties. Part 2: Magnetic Properties and Mössbauer Effect,* edited by E. Passaglia (Wiley, New York, 1973), p. 79.
[34]Z. Frait and D. Fraitová, in *Spin Waves and Magnetic Excitations,* edited by A. S. Borovik-Romanov and S. K. Sinha (Elsevier, New York, 1988), Pt. 2, p. 1.
[35]Z. Frait and D. Fraitová, Phys. Status Solidi B **154**, 363 (1989).
[36]B. Heinrich and A. S. Arrott, J. Magn. Magn. Mater. **31-34**, 669 (1983).
[37]D. S. Rodbell, Physica **1**, 279 (1965).
[38]S. M. Bhagat and H. O. Stevens, J. Appl. Phys. **39**, 1067 (1968).